Interpolated Rectangular 3-D Digital Waveguide Mesh Algorithms With Frequency Warping

Lauri Savioja, *Member, IEEE,* and Vesa Välimäki, *Senior Member, IEEE*

***Abstract*—Various interpolated three-dimensional (3-D) digital waveguide mesh algorithms are elaborated. We introduce an optimized technique that improves a formerly proposed trilinearly interpolated 3-D mesh and renders the mesh more homogeneous in different directions. Furthermore, various sparse versions of the interpolated mesh algorithm are investigated, which reduce the computational complexity at the expense of accuracy. Frequency-warping techniques are used to shift the frequencies of the output signal of the mesh in order to cancel the effect of dispersion error. The extensions improve the accuracy of 3-D digital waveguide mesh simulations enough so that in the future it can be used for acoustical simulations needed in the design of listening rooms, for example.**

***Index Terms*—Acoustic propagation, acoustic signal processing, FDTD methods, interpolation, multidimensional systems.**

I. Introduction

THE three-dimensional (3-D) digital waveguide mesh (WGM) algorithm was introduced in 1994 [2] as an extension to the formerly developed two-dimensional (2-D) WGM algorithm [3]. The technique is actually a finite difference scheme, but we still call it a digital waveguide mesh since its background lies in that tradition. The WGM approach is suitable for modeling acoustic wave propagation in restricted media, such as in musical instruments or in a room. As the 3-D WGM can be used for simulating wave propagation in a space, it turns out more important for practical applications than the 2-D WGM, which is mostly useful for physical modeling of drum membranes or other flexible vibrating surfaces. The 3-D WGM could be used as an alternative to the other techniques aiming at solving the wave equation such as the finite element method (FEM) [4] and the boundary element method (BEM) [5]. For these techniques there exist numerous practical application areas, which include the acoustical design of concert halls, churches, auditoria, listening rooms, movie theaters, cabins of various vehicles, or loudspeaker enclosures. Also simulations for testing echo cancellation and active noise control systems require the knowledge of room impulse responses.

Manuscript received June 20, 2001; revised April 30, 2003. This work was supported in part by a postdoctoral research grant from the Academy of Finland. The associate editor coordinating the review of this manuscript and approving it for publication was Dr. Walter Kellerman.

L. Savioja is with the Telecommunications Software and Multimedia Laboratory, Helsinki University of Technology (HUT), Espoo, Finland (e-mail: lauri.savioja@hut.fi; http://www.tml.hut.fi/~las/).

V. Välimäki was with Pori School of Technology and Economics, Tampere University of Technology, Tampere, Finland. He is now with the Laboratory of Acoustics and Audio Signal Processing, Helsinki University of Technology, Espoo, Finland.

Digital Object Identifier 10.1109/TSA.2003.818028

The basic version of the 3-D WGM suffers from error in wave travel speed, which depends on both direction and frequency [6]. This is called the direction-dependent dispersion error. It is the main reason why the WGM method could not have been used in many design tasks until now. To reduce the dispersion, an interpolation technique was incorporated in the 3-D WGM [7]. While the mesh was made more homogeneous in different directions, the frequency-dependence was not cured. A similar effect has been formerly observed in the interpolated 2-D WGM [8]. As a solution, a frequency-warping method can be used in the 2-D case to cut down the remaining error [9]. Alternative 3-D mesh structures, such as a tetrahedral network [6], [10], have been shown to be successful in suppressing the dispersion problem, but at the expense of a complicated tessellation of space. We believe that the usefulness of the method relies on an effortless filling of space, and thus we prefer the rectangular mesh and aim at making it an accurate and reliable method for acoustic simulations.

The contributions of this paper are a new optimized interpolation method, which is preferable to the former one, simplified versions of the interpolated mesh algorithm, and frequency-warping methods that are optimized for the new interpolated 3-D WGM. This paper is organized as follows. In Section II, we give a formulation of the 3-D WGM update rule as a finite difference scheme and present an error analysis. Section III discusses the interpolated mesh algorithm, and the optimization of the interpolation coefficients. In Section IV, we apply the frequency-warping techniques to the optimally interpolated mesh and demonstrate how the error characteristics are improved. In addition, the valid frequency range of WGM simulations is evaluated. In Section V, new interpolated sparse mesh structures are presented. In those algorithms the number of neighbors and thus also the computational load are reduced. Section VI presents results from a simulation of a rectangular space, which shows that a sufficient level of accuracy has been finally reached and that the method is ready for practical use.

II. The 3-D Digital Waveguide Mesh

The digital waveguide mesh is based on digital waveguides [11]. All these models are aimed at solving the wave equation

$$c^2\nabla^2 p = \frac{\partial^2 p}{\partial t^2} \tag{1}$$

in which p denotes the sound pressure and c is the speed of sound. In this section we describe the original rectangular mesh [2] and the methods used to analyze the dispersion error in WGM's. In addition, a couple of nonrectangular structures, such as the tetrahedral mesh [6], [10] are briefly discussed.

A. Rectangular Mesh Structure

In the original three-dimensional mesh, digital waveguides in three orthogonal directions are interconnected to each other. The final structure is a rectangular grid, in which each node has a neighbor at a unit distance in six directions, namely up, down, left, right, front, and back. The wave propagation in such a structure is governed by the following difference equation:

$$\begin{aligned} p(n+1,x,y,z) = \frac{1}{3}[&p(n,x+1,y,z)+p(n,x-1,y,z) \\ &+p(n,x,y+1,z)+p(n,x,y-1,z) \\ &+p(n,x,y,z+1)+p(n,x,y,z-1)] \\ &-p(n-1,x,y,z) \end{aligned} \quad (2)$$

where $p(n,x,y,z)$ represents the sound pressure at time step n at position (x,y,z) [2]. This structure can be analyzed by Von Neumann analysis (see, e.g., [12]), in which a spatial Fourier transform is performed to the difference scheme. Formerly this same technique has been used for 2-D meshes (see, e.g., [3], [9]). In the 3-D WGM the dispersion factor is a function of three normalized spatial frequencies ξ_x, ξ_y, and ξ_z

$$k(\xi_x,\xi_y,\xi_z) = \frac{\sqrt{3}}{2\pi\xi}\arctan\frac{\sqrt{4-b(\xi_x,\xi_y,\xi_z)^2}}{b(\xi_x,\xi_y,\xi_z)} \quad (3)$$

in which

$$b(\xi_x,\xi_y,\xi_z) = \frac{2}{3}(\cos\omega_1 cT + \cos\omega_2 cT + \cos\omega_3 cT) \quad (4)$$

where $\omega_1 = 2\pi\xi_x, \omega_2 = 2\pi\xi_y, \omega_3 = 2\pi\xi_z$, and $c = (1/\sqrt{3}T)$. The selection for speed of sound c is based on the nature of the digital waveguide mesh, and most of the results presented in the paper are valid only with the chosen speed in which waves propagate the 3-D diagonal of a unit cube in three time steps.

Fig. 1(a) shows the relative frequency error (RFE) $E(\xi_x,\xi_y,\xi_z)$ in the 3-D WGM structure. The RFE is related to the dispersion factor by the following equation:

$$E(\xi_x,\xi_y,\xi_z) = \frac{k(\xi_x,\xi_y,\xi_z)-k_{dc}}{k_{dc}}\cdot 100\% \quad (5)$$

where $k_{dc} = \lim_{\xi_x,\xi_y,\xi_z\to 0} k(\xi_x,\xi_y,\xi_z)$ in this case equals to 1. In the original rectangular 3-D mesh the maximal RFE is 23.6% on frequency band [0, 0.25].

B. Other Mesh Structures

In earlier studies, it was shown that by using interpolation it is possible to achieve wave propagation characteristics which are nearly independent of the wave propagation direction in the 2-D case [8], [9]. The same technique works also in 3-D WGM systems as shown in [7]. The interpolated rectangular mesh is discussed in detail in Section III.

There are several other applicable 3-D mesh structures in addition to the rectangular one. Their design goal has been the reduction of the dispersion error. The main problem with these is that they are more difficult to construct and analyze. For practical simulations the rectangular mesh is superior in ease of use.

The tetrahedral mesh is the oldest of the other structures that have been developed to overcome the dispersion problems occurring in the rectangular mesh [6], [10]. In this structure each node has a connection to four neighbors. The result is computationally efficient avoiding all the multiplications. But even this structure does not cure the dispersion error. The wave propagation characteristics are slightly better than in the rectangular mesh, but there still remains dispersion, which depends on the propagation directions. A thorough analysis of this tetrahedral structure can be found in the thesis by Bilbao [13]. In earlier studies it has been shown that the dispersion error can be compensated to a certain degree, only if the dispersion is independent of direction [14], [9]. Therefore this structure is not used in this study. An alternative tetrahedral structure has been presented by Campos [15]. That structure has its background in chemistry and the mesh is designed to be similar to the structure of crystal. Unfortunately, there is no analysis of dispersion error available for this structure, yet.

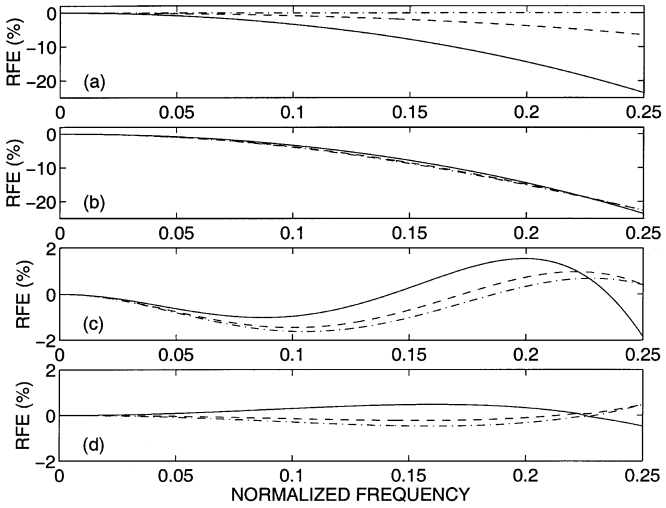

Fig. 1. Relative frequency error (RFE) in (a) the original 3-D WGM, (b) the optimally interpolated WGM ($f_{\max} = 0.25$), (c) the optimally interpolated WGM with a two-stage multiwarping ($\lambda_1 = 0.275\,389, \lambda_2 = -0.577\,291, D_1 = 2.485\,79, D_2 = 0.852\,843$), and (d) the optimally interpolated WGM with a frequency-domain warping. The curves show RFE in axial (solid line), 2-D diagonal (dashed line), and 3-D diagonal (dash-dotted line) directions. Note the different vertical scales between the first two and the last two plots.

III. Interpolated 3-D Digital Waveguide Mesh

The basic structure for the interpolated 3-D WGM is illustrated in Fig. 2. In the original rectangular mesh each node has a connection to six neighbors [see Fig. 2(a)], and that causes the direction dependent dispersion. In the interpolated mesh the number of neighbors is increased by inserting delay lines from a node to its diagonal neighbors. Finally, a node has connections of three separate type, 6 axial neighbors [Fig. 2(a)], 12 2-D diagonal neighbors [Fig. 2(b)], and eight 3-D diagonal neighbors [Fig. 2(c)], or altogether 26 neighbors as illustrated in Fig. 2(d).

The difference scheme for the interpolated 3-D WGM is [7]

$$\begin{aligned} p(n+1,x,y,z) = &\sum_{k=-1}^{1}\sum_{l=-1}^{1}\sum_{m=-1}^{1} h(k,l,m)p(n,x \\ &+k,y+l,z+m) - p(n-1,x,y,z) \end{aligned} \quad (6)$$

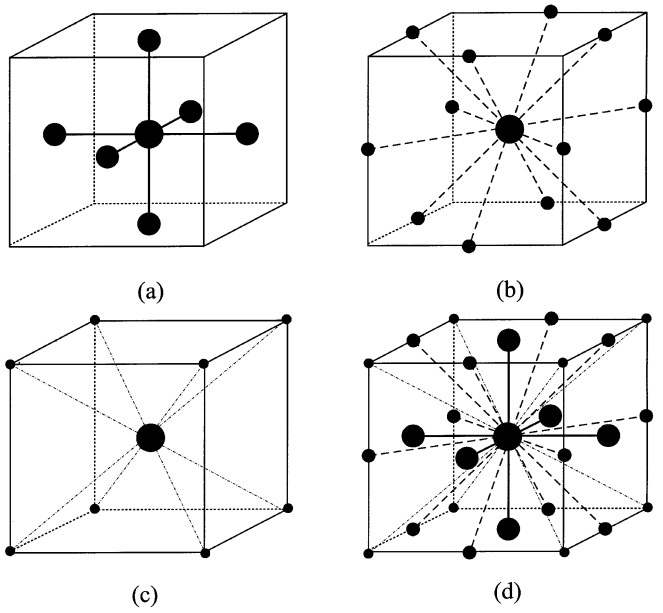

Fig. 2. Sketch of (a) six axial neighbors in the original WGM, (b) 12 2-D diagonal neighbors, (c) 8 3-D diagonal neighbors, and (d) all neighbors in the interpolated WGM. The center node is indicated with the large dot in all cases.

where $h(k,l,m)$ are the weighting coefficients for different neighbor types. In the following the coefficients are denoted as follows:

$$h(k,l,m) = \begin{cases} h_a, & \text{if } |k|+|l|+|m| = 1 \\ h_{2D}, & \text{if } |k|+|l|+|m| = 2 \\ h_{3D}, & \text{if } |k|+|l|+|m| = 3 \\ h_c, & \text{if } |k|+|l|+|m| = 0 \end{cases}. \tag{7}$$

The original rectangular mesh is obtained by setting $h_a = (1/3)$ and $h_{2D} = h_{3D} = h_c = 0$. In interpolated mesh algorithms, all or many of the above coefficients are nonzero.

A. Dispersion Analysis

For the dispersion analysis (3) is still valid, but $b(\xi_x, \xi_y, \xi_z)$ gets a new formulation

$$b(\xi_x,\xi_y,\xi_z) = 2\left[h_a \sum_{i=1}^{3} \cos \omega_i cT + h_{2D} \sum_{i=1}^{6} \cos \delta_i cT + h_{3D} \sum_{i=1}^{4} \cos \gamma_i cT + \frac{h_c}{2}\right] \tag{8}$$

where δ_i correspond to the centers of all the edges of a unit cube, and γ_i are all the corners of the spatial frequency unit cube. The values for δ_i and γ_i are shown in Table I. Equations (3) and (8) now enable the dispersion analysis for the interpolated structure.

B. Constraints for Interpolation Coefficients

The coefficient values in the interpolated three-dimensional WGM must satisfy two constraints [1]. First of all the stability criterion states that b must be real and $|b| \leq 2$. Based on (8), the maximum of b, or $b_{\max}$, is reached when $\xi \to 0$

$$b_{\max} = 2\left[3h_a + 6h_{2D} + 4h_{3D} + \frac{h_c}{2}\right] = 2. \tag{9}$$

TABLE I
VALUES FOR SPATIAL FREQUENCY COORDINATES δ_i AND γ_i REPRESENTING THE 2-D DIAGONAL AND 3-D DIAGONAL NEIGHBORS OF A NODE

$\delta_1 = \omega_1 + \omega_2$	$\gamma_1 = \omega_1 + \omega_2 + \omega_3$
$\delta_2 = \omega_1 + \omega_3$	$\gamma_2 = \omega_1 - \omega_2 + \omega_3$
$\delta_3 = \omega_2 + \omega_3$	$\gamma_3 = \omega_1 + \omega_2 - \omega_3$
$\delta_4 = \omega_1 - \omega_2$	$\gamma_4 = \omega_1 - \omega_2 - \omega_3$
$\delta_5 = \omega_1 - \omega_3$	
$\delta_6 = \omega_2 - \omega_3$	

Therefore, the coefficient for the center node can be chosen as

$$h_c = 2 - 6h_a - 12h_{2D} - 8h_{3D}. \tag{10}$$

The second constraint comes from the dispersion factor, see (3), which should equal to 1 at the zero frequency, that is

$$k_{dc} = \lim_{\xi_x,\xi_y,\xi_z \to 0} k(\xi_x,\xi_y,\xi_z) = \sqrt{12h_{2D} + 12h_{3D} + 3h_a} = 1. \tag{11}$$

From that we can solve another coefficient. Let us choose h_{3D}.

$$h_{3D} = \frac{1}{12}(1 - 12h_{2D} - 3h_a). \tag{12}$$

In the original interpolated rectangular mesh the interpolation coefficients were obtained by trilinear interpolation, which is the extension of linear interpolation in three dimensions, but the results were not accurate enough and in addition the coefficients do not satisfy the wave propagation speed constraint by (11), [7], [16]. Therefore we were obliged to search for more suitable coefficients.

Based on the previous constraints we still have two variables, h_{2D} and h_a, which can be optimized to achieve as uniform dispersion characteristics as possible in all directions.

C. Optimization of Interpolation Coefficients

The optimization of coefficients was performed such that the maximal and minimal error curves are as close to each other as possible by minimizing the difference between the two curves. The resulting coefficients are presented in Table II in which the optimization has been conducted for two separate upper limit frequencies $f_{\max}$. On the first line the error has been minimized up to $f_{\max} = 0.25$, which has been the typical limit for WGM. In the interpolated system the valid frequency range extends to 0.29 as discussed in Section IV.C, and the corresponding coefficients are shown on the second line of Table II. The maximum difference between minimum and maximum of $E(\xi_x,\xi_y,\xi_z)$ in all directions is given for each $f_{\max}$ in the rightmost column of Table II.

There still remains dispersion which increases steadily as a function of frequency, as shown in Fig. 1(b) ($f_{\max} = 0.25$). In this case the dispersion is nearly independent of the propagation direction which can be seen by comparing the RFE curves in

TABLE II
OPTIMIZED VALUES FOR INTERPOLATION COEFFICIENTS FOR TWO DIFFERENT UPPER LIMIT FREQUENCIES

f_{max}	h_a	h_{2D}	h_{3D}	h_c	Max diff. (%)
0.25	0.12052	0.03860	0.01460	0.69686	0.947
0.29	0.10861	0.03967	0.01652	0.74025	1.756

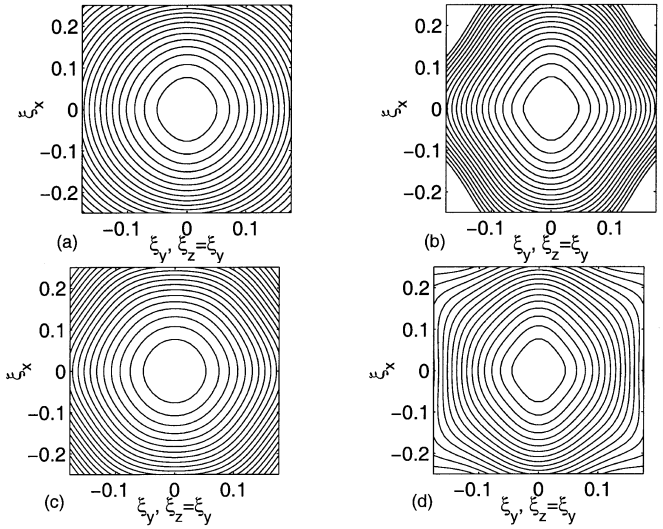

Fig. 3. Dispersion error in the full interpolated and in various sparse mesh structures as a function of spatial frequencies such that the data represents RFE in one diagonal slice of a unit cube as a function of spatial frequencies. Each contour represents a 2% decrease in speed from the center. In (a) the optimally interpolated structure is illustrated. In (b)–(d) sparse structures are shown such that (b) represents only 2-D diagonal connections, (c) depicts axial and 2-D diagonal connections, and (d) is for the structure containing axial and 3-D diagonal neighbors.

three different directions in Fig. 1(b). The dispersion in all the directions is illustrated in Fig. 3(a).

IV. APPLYING FREQUENCY WARPING TO REDUCE THE DISPERSION ERROR

There are two different principles to apply the frequency warping. In our previous studies concerning the 2-D WGM, we have utilized warping in the time domain [14], [9]. In the case of the 3-D WGM more accurate results may be obtained by warping in the frequency domain. In the following we show results for both techniques.

A. Frequency Warping in the Time Domain

Since the error curves are smooth and nearly the same in all the directions [see Fig. 1(b)], it is possible to apply a frequency warping to reduce the dispersion [9]. The warping is performed to the input and output signals of the mesh [9] using a warped FIR filter [17]. It is an FIR filter in which each unit delay element has been replaced with a first-order allpass filter having the transfer function

$$A(z) = (z^{-1} + \lambda)/(1 + \lambda z^{-1}). \tag{13}$$

There are various techniques to find an optimal value for the warping coefficient λ [9]. With a single warping ($\lambda = -0.253\,059$) the best result was 3.8% maximal error for $f_{\max} = 0.25$. The error can still be reduced by applying the *multiwarping* technique in which multiple signal resampling and frequency warping operations are cascaded [18], [19]. By using multiwarping which contains two warping and two signal resampling operations, a maximal error of 1.8% is achieved. The corresponding error curves are given in Fig. 1(c).

The warping techniques discussed in this article are suitable for offline processing such that both the input and output signals of a mesh are processed. Lately there have been suggestions also on implementing the warping inside a mesh structure thus enabling online warping [20], [21].

B. Frequency Warping in the Frequency Domain

Warping in the frequency domain is made by nonuniform resampling of the Fourier transformed signal [22], [23, p. 13]. In this case, the resampling intervals are determined by the relative wave propagation speed curves. The applied warping curve corresponds to average of RFE's shown in Fig. 1(b) thus minimizing the maximal error. Note that the Fourier transform must be performed with a large number of datapoints so that the interpolation of spectral data causes only minimal error. Due to the nature of the transform, the frequency response is complex. Therefore the interpolation has to be applied to both the real and the imaginary parts thus preserving both the magnitude and phase of the response. By this technique the maximal error is reduced to 0.474%, as illustrated in Fig. 1(d). That error is one half of the maximal difference presented for $f_{\max} = 0.25$ in Table II.

C. Extending the Frequency Range

Next, we discuss the question of the upper frequency limit of the interpolated and warped WGM simulations. It is known that the limiting frequency in the case of the original waveguide mesh is 0.25, and above that frequency only mirror images of lower frequencies occur [3], [24]. However, when interpolation and frequency-warping methods are used, it is no longer obvious what the highest frequency is. In the following, we demonstrate how it is possible to extend the frequency range of digital waveguide mesh simulations. A similar study has been presented previously for the 2-D case [18].

Fig. 4 shows the mapping of the original normalized frequencies to the frequencies occurring on the mesh in the case of the original [Fig. 4(a)] and optimally interpolated meshes, when the frequency limit has been set to 0.25 [in Fig. 4(b)] and 0.29 [in Fig. 4(c)]. The maximum value of all axial mapping

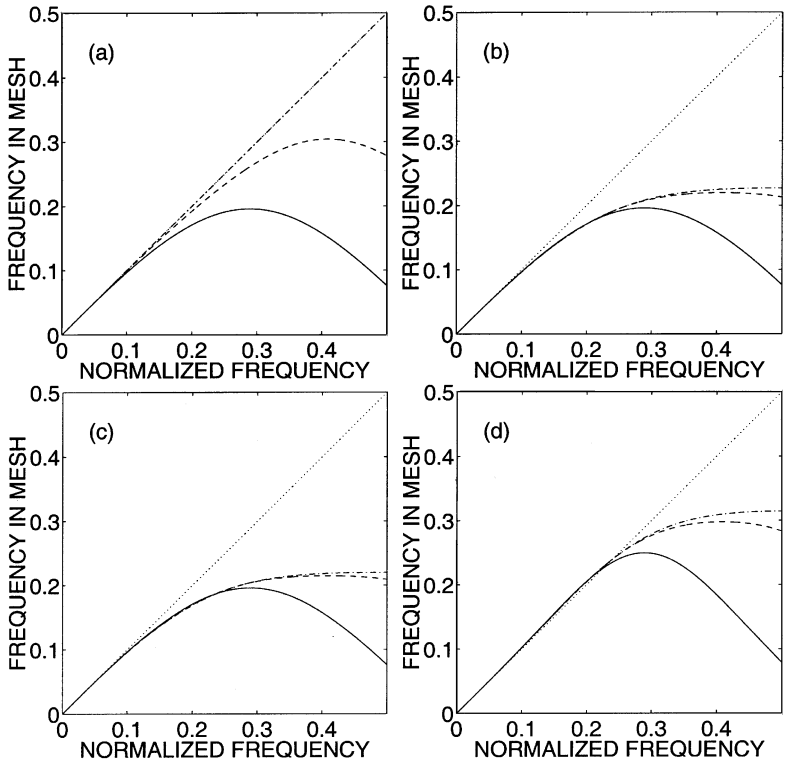

Fig. 4. Mapping of frequencies in the (a) original, (b) optimally interpolated (up to 0.25), and (c) another optimally interpolated (up to 0.29) waveguide mesh together with (d) warped mapping for case (b). The axial direction is shown with the solid, the 2-D diagonal direction with the dashed, and the 3-D diagonal with dash-dotted line. The dotted line indicates the desired ideal mapping function $(y = x)$.

curves without warping is 0.196, and it occurs at normalized frequency 0.29. This appears to be the highest frequency that can be simulated using the interpolated rectangular 3-D digital waveguide meshes. Frequency warping could at its best shift the mesh frequencies so that 0.29 would again occur at the right frequency. Assuming ideal frequency warping, the remaining error is caused by the differences between different directions. Note that in 2-D WGM similar behavior is observed, but in the 2-D case the maximum frequency is 0.35 [18].

As an example, we display in Fig. 4(d) the frequency mapping of the warped interpolated mesh optimized up to the normalized frequency 0.25. It can be seen that both the axial and diagonal frequency mappings follow the ideal mapping function [dotted line in Fig. 4(d)] well until about 0.25. Above this frequency, also the difference between the diagonal and axial properties of the mesh begins to increase substantially, and it is impossible to extend the bandwidth much higher. However, it would be possible to warp the interpolated mesh that has been optimized up to 0.29 [see Fig. 4(c)], and then it would be feasible to obtain a reasonably good accuracy up to 0.29.

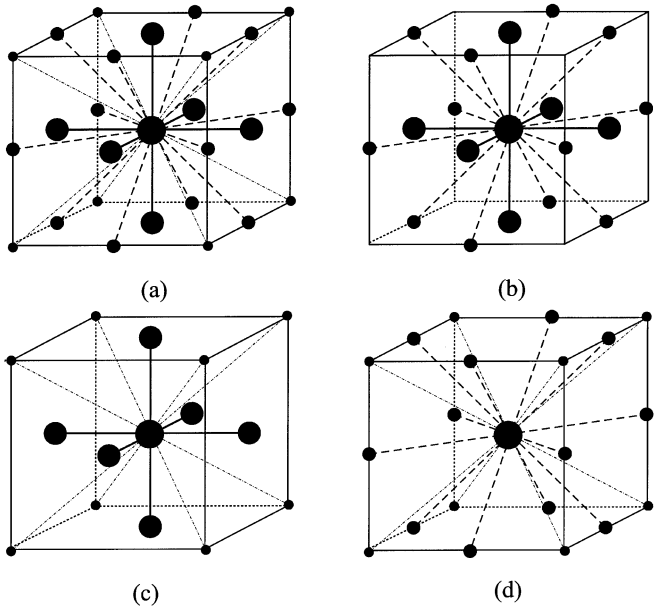

Fig. 5. Various sparse mesh structures utilizing different number of neighbors: (a) all the neighbors are involved, (b) axial and 2-D diagonal connections, (c) axial and 3-D diagonal connections, and (d) 2-D and 3-D diagonal connections. The center node is indicated with the large dot in all cases.

V. Sparse Interpolated Mesh Algorithms

In the interpolated structure discussed above there are 27 connections from each node: 26 connections to the neighbors and a delayed feedback connection to the node itself [see (6)]. When compared to the original mesh with six connections the number of required operations is nearly five times larger. In the following, we study some compromises in which the number of connections is reduced. We have tested various sparse structures by setting some of the interpolation coefficients h_a, h_{2D}, or h_{3D} to zero, and performing the optimization of interpolation and warping coefficients in series. All the resulting structures are illustrated in Figs. 2 and 5. The obtained RFEs are shown in Table III. All the optimizations were done up to $f_{\max} = 0.25$.

TABLE III
OPTIMIZED VALUES FOR INTERPOLATION COEFFICIENTS AND CORRESPONDING MAXIMAL RFE FOR DIFFERENT STRUCTURES SUCH THAT A STANDS FOR AXIAL DIRECTIONS, 2D FOR 2D-DIAGONALS, AND 3D FOR 3-D DIAGONAL DIRECTIONS. IN THE FIRST LINE, THE RESULTS FOR THE COMPLETE STRUCTURE WITH 26 NEIGHBORS ARE SHOWN. THE FIGURE RFE (SW) STANDS FOR THE RELATIVE FREQUENCY ERROR WITH SINGLE WARPING, AND THE RFE (FDW) IS FOR THE WARPING IN THE FREQUENCY DOMAIN

Structure	Fig.	h_a	h_{2D}	h_{3D}	h_c	RFE (SW)	RFE (FDW)
All	2(d)	0.12052	0.03860	0.01460	0.69686	3.783%	0.474%
A	2(a)	0.33333	0.00000	0.00000	0.00000	16.314%	11.793%
2D	2(b)	0.00000	0.08333	0.00000	1.00000	13.043%	4.858%
3D	2(c)	0.00000	0.00000	0.08333	1.33333	37.332%	13.159%
A2D	5(b)	0.09174	0.06040	0.00000	0.72479	4.012%	1.380%
A3D	5(c)	0.15261	0.00000	0.04518	0.72288	4.761%	2.376%
2D3D	5(d)	0.00000	0.09502	-0.01168	0.95327	10.102%	4.005%

The first line of Table III can be used as a reference since it stands for the complete interpolated mesh having 27 connections. The next three lines represent cases in which two of the coefficients have been forced to zero corresponding to structures 2(a)–(c). In these cases there is no need for optimization of coefficients since there are no more degrees of freedom but all the values for the remaining coefficients come directly from the constraints (10) and (12). Note that the structure having $h_a = 1/3$ is the original rectangular 3-D digital waveguide mesh.

Fig. 3(b)–(d) illustrates the dispersion error in various sparse structures such that in (b) only the 2-D diagonals have connections to the center node, in (c) both the axial and 2-D diagonal neighbors are utilized, and in (d) axial and 3-D diagonals are connected. The figure shows dispersion in all the directions such that the error is calculated on a 2-D diagonal surface of a unit cube of spatial frequencies ξ_x, ξ_y, and ξ_z. Note that we show the dispersion factor up to spatial frequency radius $\xi = 0.25$: In the x direction this implies 0.25 and in the $y = z$ diagonal direction $0.25/\sqrt{2} = 0.1768$. It is interesting to see that the mesh consisting of 12 2-D axial neighbors yields pretty low RFE of 4.9% with warping in the frequency domain. The corresponding error contours without frequency warping are shown in Fig. 3(b).

The last three lines of Table III present results for the cases in which only one of the coefficients is missing. These structures are illustrated in Fig. 5. The results show that the case in which the axial and 2-D diagonal connections are utilized [Fig. 5(b)] is quite similar to the full structure [Fig. 5(a)] but the number of neighbors has been decreased from 26 to 18.

The number of required operations in each structure is presented in Table IV. The cases are the same as in Table III. In the calculation of the total computational load, additions and multiplications are considered to cause an equal load. It is interesting to note that in the case of only 2-D diagonal neighbors the factor $h_c = 1$ thus avoiding one multiplication.

As a conclusion, we suggest that for applications in which the computational load is more important than accuracy some reduced structure can be utilized. The most cost effective structures seem to be the one having only 2-D diagonal connections [see Fig. 2(b)], and the one having both axial and 2-D diagonal neighbors [see Fig. 5(a)]. They have RFEs of 4.9% and 1.4%, respectively, with warping in the frequency domain.

TABLE IV
COMPUTATIONAL LOAD OF VARIOUS MESH STRUCTURES. IN THE TOTAL LOAD THE ADDITIONS AND MULTIPLICATIONS ARE CONSIDERED EQUALLY EXPENSIVE

Structure	Adds	Muls	Total
All	26	4	100.0%
A	6	1	23.3%
2D	12	1	43.3%
3D	8	2	33.3%
A2D	18	3	70.0%
A3D	14	3	56.7%
2D3D	20	3	76.7%

VI. SIMULATION EXAMPLE OF A CUBE AND COMPARISON TO THE OTHER TECHNIQUES

As an example an ideal cube was simulated. The mesh consisted of $8 \times 8 \times 8 = 512$ nodes and the walls had a reflection coefficient -1. Hence, we did not have to perform any interpolation or filtering at the boundaries. An impulse excitation was located near one corner, and the receiver was at the opposite one. In the simulation 3298 time steps were calculated and the magnitude response was computed by Fourier transforming the obtained impulse response. The simulation was run with four different variations of the algorithms, and the results are illustrated in Fig. 6. In all figures the dashed line stands for the analytically solved magnitude response. In the original rectangular mesh, presented in Fig. 6(a), some of the modes are at correct locations while others are too low. Both the optimally interpolated mesh with multiwarping [Fig. 6(b)] and the optimally interpolated mesh with warping in the frequency domain [Fig. 6(c)] enhance the situation remarkably. It is easy to see that the most accurate result is obtained when the warping is performed in the frequency domain, as already shown in Section IV-B. The most accurate ofthe sparse constructions is the one having connections to the axial and 2-D diagonal neighbors illustrated in Fig. 5(b). The simulation result given by this with warping in the frequency domain is shown in Fig. 6(d). In all the simulations the

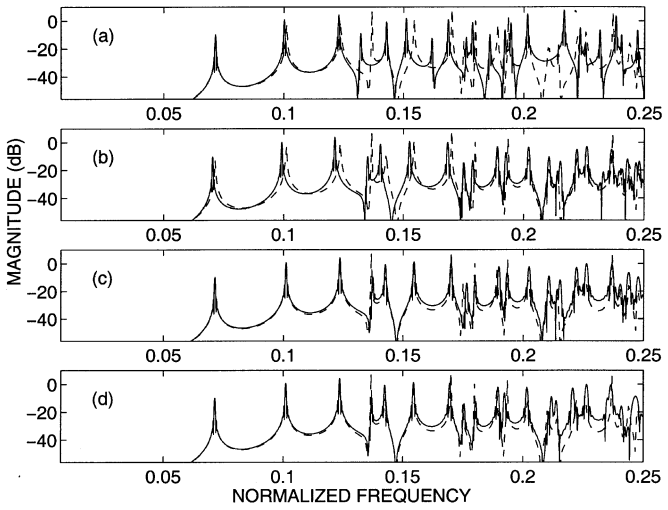

Fig. 6. Cubic space is simulated and a transfer function is calculated (a) with the original rectangular mesh, (b) with the optimally interpolated mesh applying multiwarping, (c) with the optimally interpolated mesh using warping in the frequency domain, and (d) with the sparse structure containing axial and 2-D diagonal neighbors and warping in the frequency domain. In all the interpolated cases the optimization has been performed upto $f_{\max} = 0.25$. The solid line represents the simulation result and the dashed line is the analytical solution.

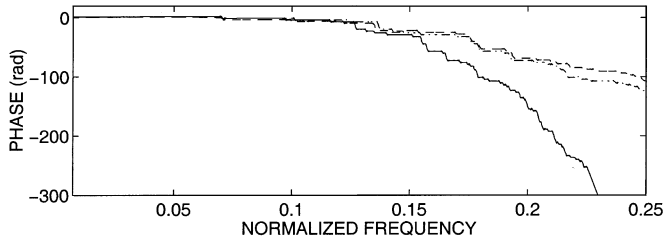

Fig. 7. Various phase responses of the simulation result obtained with the optimally interpolated mesh. The solid line represents the phase without any warping, the dashed line is the phase after multiwarping, and the dash-dotted line shows it after warping in the frequency domain.

obtained RFEs are in good agreement with the analytically calculated curves illustrated in Fig. 1.

Fig. 7 shows the effect of frequency warping into the phase response of one simulation obtained with the optimally interpolated mesh. The solid line represents the phase without warping, and the dashed line shows the phase after warping in the time domain corresponding to the magnitude response drawn with the solid line in Fig. 6(b). The dash-dotted line stands for warping in the frequency domain, and the corresponding magnitude response is illustrated with the solid line in Fig. 6(c). In the interpolated mesh all the high frequency modes are shifted toward the lower frequencies, and that is seen as a steep slope in the nonwarped phase curve in Fig. 7. Warping is utilized to compensate for that error and in both of the warped phase responses the slopes are more modest. There are some variations between the time-domain and frequency-domain warped phase responses, but the differences correspond well to the analytically calculated RFEs illustrated in Figs. 1(c) and (d).

This simulation example is quite simple, but due to computational simplicity of the technique much larger meshes up to tens of millions of nodes are possible, as well. The main difference between the WGM and the element methods is that both of the element methods require inversion of a large matrix, and that is not needed in finite difference methods. Therefore the WGM is computationally easier than FEM and BEM. The power of FEM and BEM lies in their ability to use arbitrary shaped elements, but that limits the possibility to obtain uniform dispersion properties, which is a strength in our technique. This results in the ability to utilize the frequency warping technique with WGM to compensate the dispersion error up to a certain degree. In addition, the WGM is more intuitive and easier to implement than the element methods.

VII. Conclusion

An optimally interpolated 3-D digital waveguide mesh with rectangular structure was presented. By applying interpolation to increase the number of propagation directions, nearly direction independent wave propagation characteristics are obtained. The remaining dispersion can be reduced by frequency warping, which can be performed either in the time domain or in the frequency domain. The relative frequency error is reduced to less than 0.5% when the warping is done in the frequency domain. The new method improves the frequency accuracy of the original 3-D mesh remarkably. In addition, sparse versions of the interpolated digital waveguide mesh were derived and tested. In the future, research efforts should focus on accurate implementation of various boundary conditions in the mesh.

References

[1] L. Savioja and V. Välimäki, "Interpolated 3-D digital waveguide mesh with frequency warping," in *Proc. Int. Conf. Acoust., Speech, Signal Processing*, vol. 5, Salt Lake City, UT, May 15–19, 2001, pp. 3345–3348.

[2] L. Savioja, T. Rinne, and T. Takala, "Simulation of room acoustics with a 3-D finite difference mesh," in *Proc. Int. Computer Music Conf.*, Aarhus, Denmark, Sept. 12–17, 1994, pp. 463–466.

[3] S. Van Duyne and J. O. Smith, "The 2-D digital waveguide mesh," *Proc. IEEE Workshop on Applications of Signal Processing to Audio and Acoustics*, Oct. 1993.

[4] A. Craggs, "Acoustic modeling: Finite element method," in *Encyclopedia of Acoustics*, M. J. Crocker, Ed. New York: Wiley, 1997, vol. 1, ch. 14, pp. 165–172.

[5] A. F. Seybert and T. W. Wu, "Acoustic modeling: Boundary element methods," in *Encyclopedia of Acoustics*, M. J. Crocker, Ed. New York: Wiley, 1997, vol. 1, ch. 15, pp. 173–183.

[6] S. Van Duyne and J. O. Smith, "The tetrahedral digital waveguide mesh," *Proc. IEEE Workshop on Applications of Signal Processing to Audio and Acoustics*, Oct. 1995.

[7] L. Savioja, "Improving the three-dimensional digital waveguide mesh by interpolation," in *Proc. Nordic Acoustical Meeting*, Stockholm, Sweden, Sept. 7–9, 1998, pp. 265–268.

[8] L. Savioja and V. Välimäki, "Improved discrete-time modeling of multi-dimensional wave propagation using the interpolated digital waveguide mesh," in *Proc. IEEE Int. Conf. Acoust., Speech, Signal Processing*, vol. 1, Munich, Germany, Apr. 19–24, 1997, pp. 459–462.

[9] ——, "Reducing the dispersion error in the digital waveguide mesh using interpolation and frequency-warping techniques," *IEEE Trans. Speech Audio Processing*, vol. 8, pp. 184–194, Mar. 2000.

[10] S. Van Duyne and J. O. Smith, "The 3D tetrahedral digital waveguide mesh with musical applications," in *Proc. Int. Computer Music Conf.*, Hong Kong, Aug. 19–24, 1996, pp. 9–16.

[11] J. O. Smith, "Principles of digital waveguide models of musical instruments," in *Applications of Digital Signal Processing to Audio and Acoustics*, M. Kahrs and K. Brandenburg, Eds. Boston, MA: Kluwer, 1997, ch. 10, pp. 417–466.

[12] J. Strikwerda, *Finite Difference Schemes and Partial Differential Equations*. New York: Chapman & Hall, 1989.

[13] Wave and Scattering Methods for the Numerical Integration of Partial Differential Equations, S. Bilbao. (2001). [Online]. Available: http://ccrma-www.stanford.edu/~bilbao/

[14] L. Savioja and V. Välimäki, "Reduction of the dispersion error in the triangular digital waveguide mesh using frequency warping," *IEEE Signal Processing Lett.*, vol. 6, pp. 58–60, Mar. 1999.
[15] G. Campos and D. Howard. A parallel 3D digital waveguide mesh model with tetrahedral topology for room acoustic simulation. presented at COST G-6 Conf. Digital Audio Effects. [Online]. Available: http://profs.sci.univr.it/~dafx/DAFx-final-papers.html
[16] Modeling Techniques for Virtual Acoustics, L. Savioja. (1999). [Online]. Available: http://www.tml.hut.fi/~las/publications
[17] A. Oppenheim, D. Johnson, and K. Steiglitz, "Computation of spectra with unequal resolution using the fast Fourier transform," *Proc. IEEE*, vol. 59, pp. 299–301, Feb. 1971.
[18] V. Välimäki and L. Savioja. Interpolated and warped 2-D digital waveguide mesh algorithms. presented at COST G-6 Conf. Digital Audio Effects. [Online]. Available: http://profs.sci.univr.it/~dafx/DAFx-final-papers.html
[19] L. Savioja and V. Välimäki, "Multiwarping for enhancing the frequency accuracy of digital waveguide mesh simulations," *IEEE Signal Processing Lett.*, vol. 8, pp. 134–136, May 2001.
[20] F. Fontana and D. Rocchesso, "Online correction of dispersion error in 2D waveguide meshes," in *Proc. Int. Computer Music Conf.*, Berlin, Germany, Aug. 2000, pp. 78–81.
[21] S. Stoffels. Full mesh warping techniques. presented at COST G-6 Conf. Digital Audio Effects. [Online]. Available: http://profs.sci.univr.it/~dafx/DAFx-final-papers.html
[22] J. O. Smith, "Techniques for Digital Filter Design and System Identification with Application to the Violin," Ph.D. Thesis, Elect. Eng. Dept., Stanford University, Stanford, CA, June 1983.
[23] J.-M. Jot, V. Larcher, and O. Warusfel, "Digital signal processing issues in the context of binaural and transaural stereophony," in *The 98th Audio Engineering Society (AES) Convention, Preprint 3980*, Paris, France, Feb. 1995.
[24] F. Fontana and D. Rocchesso, "Signal-theoretic characterization of waveguide mesh geometries for models of two-dimensional wave propagation in elastic media," *IEEE Trans. Speech Audio Processing*, vol. 9, pp. 152–161, Feb. 2001.

Lauri Savioja (M'03) was born in Turku, Finland, in 1966. He studied computer science and acoustics and received the M.S. degree in technology (1991), the Licentiate of Science degree in technology (1995), and the Doctor of Science degree in technology (1999) from the Department of Computer Science, Helsinki University of Technology (HUT), Espoo, Finland.

Currently he is a Professor with the Laboratory of Telecommunications Software and Multimedia with HUT. His research interests include virtual reality, room acoustics, and physical modeling of musical instruments.

Dr. Savioja is a member of the Audio Engineering Society, ACM, and the Acoustical Society of Finland.

Vesa Välimäki (S'90–M'92–SM'99) was born in Kuorevesi, Finland, in 1968. He received the M.S. degree in technology, the Licentiate of Science degree in technology, and the Doctor of Science degree in technology, all in electrical engineering from Helsinki University of Technology (HUT), Espoo, Finland, in 1992, 1994, and 1995, respectively.

He was with the HUT Laboratory of Acoustics and Audio Signal Processing from 1990 to 2001. In 1996, he was a Postdoctoral Research Fellow with the University of Westminster, London, U.K. During the academic year 2001–2002, he was Professor of signal processing at the Pori School of Technology and Economics, Tampere University of Technology (TUT), Pori, Finland. In August 2002 he returned to HUT, where he is currently Professor of audio signal processing. He was appointed Docent in signal processing at the Pori School of Technology and Economics, TUT, in 2003. His research interests are in the areas of musical signal processing and filter design.

Dr. Välimäki is a senior member of the IEEE Signal Processing Society and is a member of the Audio Engineering Society, the International Computer Music Association, the Acoustical Society of Finland, and the Finnish Musicological Society. He was secretary of the IEEE Finland Section in 2000 and 2001.